Int. J. Heat Mass Transfer. Vol. 6, pp. 193–210. Pergamon Press 1963. Printed in Great Britain.

EFFECT OF DISCONTINUITY OF SURFACE CATALYCITY ON BOUNDARY LAYER FLOW OF DISSOCIATED GAS

P. M. CHUNG,† S. W. LIU‡ and H. MIRELS§

Aerodynamic and Propulsion Research Laboratory, Aerospace Corporation, El Segundo, California

(*Received* 5 *June* 1962)

Abstract—The catalytic recombination of atoms along a surface with a discontinuous variation of the surface catalytic activity is studied. The catalycity is considered to have a discrete jump from either zero or infinity to an arbitrary but constant value at a given location. Highly cooled hypersonic laminar boundary layers are considered for general two-dimensional and axisymmetric bodies. Two approaches are used in the study: a Volterra integral equation which is solved by both a series method and a numerical method and a modified Pohlhausen integral method.

The effect of a non-catalytic up-stream surface on the heat transfer to down-stream surfaces with a finite catalycity is discussed. Also, a method is advanced to increase the sensitivity of a differential catalytic gage used for the determination of local atom concentrations of high temperature experimental facilities.

NOMENCLATURE

A, parameter defined by (27);
a_n, expansion coefficients defined in (31);
b_n, expansion coefficients defined in (32);
C, $\rho\mu/\rho_e\mu_e$;
$\bar{C}$, $\rho\mu/(\rho_e\mu_e)_s$;
c_p, specific heat at constant pressure;
D, diffusion coefficient;
F, atom concentration integral defined by (50);
G, parameter defined by (60);
$\bar{G}$, parameter defined by (55);
h, frozen total enthalpy defined by (6);
h_R, heat of recombination of atoms;
k_w, specific constant for catalytic surface reaction;
L, reference length in general; nose radius for spherical nose;
m, α/α_e;
n, integer;
Pr, Prandtl number;
p, pressure;
q, heat transfer to surface/unit time/unit area;
Re, $u_\infty x_0/\nu_{es}$;
r, distance from axis of symmetry to a point on the surface;
Sc, Schmidt number;
s, streamwise variable defined by (7);
T, absolute temperature;
t, variable defined by (7);
U, $u/u_e = \partial\psi/\partial t$;
u, x-component of velocity;
V, $-\partial\psi/\partial s$;
v, y-component of velocity;
x, streamwise distance along the surface;
y, distance normal to surface;
z, mathematical dummy variable.

Greek symbols

α, mass fraction of atoms;
β_s, $(L/u_\infty)(du_e/dx)_s$ for sphere;
Γ, gamma function;
γ, $\begin{cases} 1 \text{ when } k_w = \infty \text{ for } s \leqq s_0 \\ 0 \text{ when } k_w = 0 \text{ for } s \leqq s_0; \end{cases}$
Δ, non-dimensional momentum boundary layer thickness defined by (47);
Δ_m, non-dimensional diffusion boundary layer thickness defined by (50);
δ, modified momentum boundary layer thickness defined by (48);
$\hat{\delta}$, momentum boundary layer thickness;
δ_m, modified diffusion boundary layer thickness defined by (50);

† Head, Heat Transfer Section.
‡ Staff Scientist.
§ Head, Advanced Propulsion and Fluid Mechanics Department.

δ_m, diffusion boundary layer thickness;
η, variable defined by (50);
θ, half-wedge angle or half-cone angle;
λ, variable defined by (29);
μ, absolute viscosity;
ν, kinematic viscosity;
ξ, s/s_o;
ρ, density;
Φ, form factor defined by (27);
ϕ, variable defined by (39);
ψ, stream function defined by (11);
Ω, function defined by (66).

Superscripts

ϵ, $\begin{cases} 1 \text{ for axisymmetric bodies} \\ 0 \text{ for two-dimensional bodies;} \end{cases}$
$( )'$, total differentiation with respect to ξ.

Subscripts

c, due to convection;
d, due to diffusion and recombination of atoms;
e, edge of boundary layer;
i, ith species;
j, location at which (62) and (63) are joined;
o, location at which k_w varies from either zero or ∞ to an arbitrarily constant value discontinuously;
s, stagnation point or leading edge;
T, total value;
un, uniform k_w from leading edge or stagnation point;
w, wall;
2, molecule;
∞, free stream.

1. INTRODUCTION

THE gases in the immediate vicinity of hypersonic vehicles are usually dissociated. The dissociated radicals tend to recombine in the gas or on the surface as the gas flows over the body. When the gas contains a large amount of radicals, the heat transfer to the surface is greatly affected by the rate at which the recombination is taking place. A study of the factors which govern the recombination process is, therefore, very important in the analysis of such heat transfer.

Extensive study has been carried out on non-equilibrium boundary layer and surface reactions by different authors [1–11]. In the light of [2–4], it can be seen that the gas-phase recombination may be nearly frozen for many flight conditions of hypersonic vehicles and for extensive regime of test conditions in high temperature experimental facilities. Under such circumstances, the chemical energy of the dissociated radicals participates in the heat transfer only through the surface recombination.

The subject of catalytic surface recombination in the boundary layer flow of frozen dissociated gas has been analysed extensively [5–11]. However, all the previous analyses have been confined to the case in which the catalytic efficiency of the surface is invariant along the surface. In practice, the catalytic efficiency of the surface may vary in some arbitrary manner either due to the variation of surface temperature or the surface material. With a continuous variation of surface temperature, the catalytic efficiency also varies continuously. On the other hand, when the surface is made of different materials located adjacently, the catalytic efficiency will have a discontinuous variation.

In the present paper methods of solution are presented for treating discontinuous variations of surface catalytic efficiency. In the specific examples presented, attention is limited to the cases in which a surface of an arbitrary, but constant, catalytic efficiency is located down stream of a leading edge or stagnation region which is either a perfect catalyst or a total non-catalyst.

The governing laminar boundary layer equations are first derived for the hypersonic flow over two-dimensional and axisymmetric bodies with a discontinuity in the surface catalycity. The general behavior and the method of solution of the equations are discussed. The specific problem of catalytic reaction taking place along the surfaces following a non-catalytic surface is then solved for a flat plate, wedges, and cones and for a hemisphere. Finally, the implications of these solutions with regard to typical applications are discussed.

The boundary layer is considered to be comprised of a frozen dissociated gas throughout the analysis.

Two of the more important applications of the present analysis arise as follows.

(a) Consider that a non-catalytic surface material is used locally to reduce the maximum local heat transfer such as near a leading edge or a stagnation point. The present analysis, then, gives the effect of the upstream surface chemical condition on the heat transfer to the downstream surface when its catalytic efficiency is different from that of the upstream surface.

(b) The second application is associated with the construction of catalytic gages for the diagnostics (measurement of local atom concentrations) of high temperature experimental facilities. It will be shown later that, in many cases, it is advantageous to locate the catalytic gage surface away from a leading edge or a stagnation point and, at the same time, use a non-catalytic material for the surfaces upstream of the gage surface. The present analysis gives the heat transfer along the gage surface which can then be used to deduce the free stream concentration of radicals.

2. TRANSFORMATION OF BOUNDARY LAYER EQUATIONS

Consider the boundary layer flow around two-dimensional and axisymmetric bodies (see Fig. 1 for the physical models). The fluid is considered to be a partially dissociated diatomic gas of constant Prandtl and Schmidt numbers, and it is assumed to be chemically frozen in this state throughout the entire flow field under consideration. The governing boundary layer equations are:

(a) Continuity

$$\frac{\partial \rho u r^{\epsilon}}{\partial x} + \frac{\partial \rho v r^{\epsilon}}{\partial y} = 0. \tag{1}$$

(b) Momentum

$$\rho u \frac{\partial u}{\partial x} + \rho v \frac{\partial u}{\partial y} = \frac{\partial}{\partial y}\left(\mu \frac{\partial u}{\partial y}\right) - \frac{\mathrm{d}p}{\mathrm{d}x}. \tag{2}$$

(c) Frozen total energy

$$\rho u \frac{\partial h}{\partial x} + \rho v \frac{\partial h}{\partial y} = \frac{\partial}{\partial y}\left(\frac{\mu}{Pr}\frac{\partial h}{\partial y}\right) + \frac{\partial}{\partial y}\left[\mu\left(1 - \frac{1}{Pr}\right)\frac{\partial}{\partial y}\left(\frac{u^2}{2}\right)\right]. \tag{3}$$

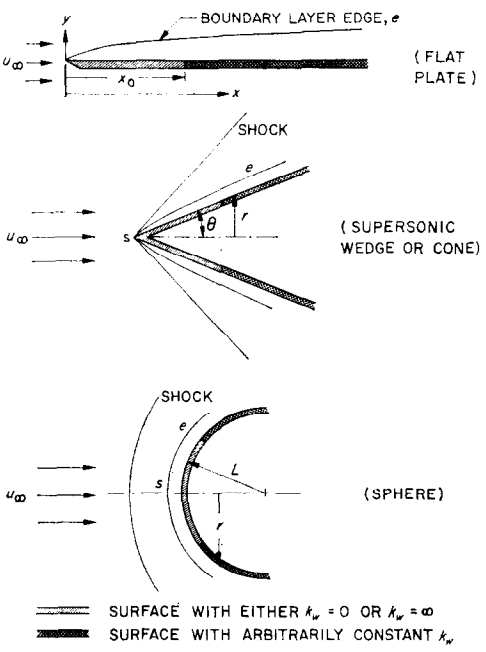

FIG. 1. Flow configurations considered.

(d) Diffusion of atoms

$$\rho u \frac{\partial a}{\partial x} + \rho v \frac{\partial a}{\partial y} = \frac{\partial}{\partial y}\left(\frac{\mu}{Sc}\frac{\partial a}{\partial y}\right). \tag{4}$$

(e) Mass fraction of molecules

$$a_2 = 1 - a \tag{5}$$

where

$$h = \sum (a_i \int_0^T c_{pi}\,\mathrm{d}T) + \frac{u^2}{2}. \tag{6}$$

As discussed in [11], the boundary condition associated with the surface reaction usually does not permit a complete similarity solution of the governing equations. Particularly, in the present case of discontinuity of surface catalycity, it is very unlikely that a similarity solution exists. With this in mind, the general transformation technique used in [11] will be first applied on the governing equations, (1–4), to simplify them.

A set of independent variables is defined as

$$s = \int_0^x \bar{C} u_e r^{2\epsilon}\,\mathrm{d}x$$

$$t = u_e r^{\epsilon} \int_0^y \frac{\rho}{\rho_{es}}\,\mathrm{d}y \tag{7}$$

where

$$\bar{C} = \frac{\rho\mu}{(\rho_e\mu_e)_s} = \left(\frac{\rho\mu}{\rho_e\mu_e}\right)\frac{\rho_e\mu_e}{(\rho_e\mu_e)_s} = C\frac{\rho_e\mu_e}{(\rho_e\mu_e)_s}. \quad (8)$$

The local $\rho\mu$-ratio, C, will be considered to be a suitably chosen constant. For instance, we may let

$$C = \left[\left(\frac{\rho_w\mu_w}{\rho_e\mu_e}\right)_s\right]^{0.2} \quad (9)$$

for low local Mach numbers in accordance with the suggestion of [12]. A study of [12] and [13] shows that the effect of assuming a constant C on surface phenomena, such as heat transfer and diffusion to the wall, may be at most of the order of 5 to 10 per cent.

Next, a set of dependent variables is defined in terms of the stream function ψ as

$$U = \frac{\partial\psi}{\partial t}$$

$$V = -\frac{\partial\psi}{\partial s}. \quad (10)$$

Where ψ satisfies the continuity equation identically, i.e.,

$$\rho u r^\epsilon = \rho_{es}\frac{\partial\psi}{\partial y}$$

$$\rho v r^\epsilon = -\rho_{es}\frac{\partial\psi}{\partial x}. \quad (11)$$

The governing equations (1–5) become:

(a) Continuity

$$\frac{\partial U}{\partial s} + \frac{\partial V}{\partial t} = 0. \quad (12)$$

(b) Momentum

$$U\frac{\partial U}{\partial s} + V\frac{\partial U}{\partial t} = \nu_{es}\frac{\partial^2 U}{\partial t^2} + \frac{1}{u_e}\frac{\mathrm{d}u_e}{\mathrm{d}s}\left(\frac{\rho_e}{\rho} - U^2\right). \quad (13)$$

(c) Frozen total energy

$$U\frac{\partial h}{\partial s} + V\frac{\partial h}{\partial t} = \frac{\nu_{es}}{Pr}\frac{\partial^2 h}{\partial t^2} + \nu_{es}u_e^2\left(1 - \frac{1}{Pr}\right)\frac{\partial^2}{\partial t^2}\left(\frac{U^2}{2}\right). \quad (14)$$

(d) Diffusion of atoms

$$U\frac{\partial\alpha}{\partial s} + V\frac{\partial\alpha}{\partial t} = \frac{\nu_{es}}{Sc}\frac{\partial^2\alpha}{\partial t^2}. \quad (15)$$

(e) Mass fraction of molecules

$$\alpha_2 = 1 - \alpha. \quad (16)$$

The reader is referred to [11] for a more detailed derivation of (12–16).

The last term of (13) is zero for a flat plate or wedge and cone in supersonic flow since there is no pressure gradient. Also, according to [13], the last term may be neglected for a highly cooled boundary layer ($\rho_e/\rho_w \ll 1$) with pressure gradient. Equation (13), therefore, becomes for a flat plate, wedge, cone, and for a highly cooled blunt body:

$$U\frac{\partial U}{\partial s} + V\frac{\partial U}{\partial t} = \nu_{es}\frac{\partial^2 U}{\partial t^2}. \quad (17)$$

As a consequence of assumption (8), the momentum equation (17) and the diffusion equation (15) are no longer coupled to the energy equation. The solution of energy equation (14) depends on the momentum equation and this may be found elsewhere, [13]. Now it is seen that the boundary layer equations to be solved in the present analysis are the simplified continuity, momentum, and diffusion equations of (12), (17), and (15). Once the solution of the diffusion equation is known, the total heat transfer distribution can be obtained by the use of the solution of the frozen energy [see (65)] and the diffusion equations as

$$q_T = q_c + q_d, \quad (18)$$

where

$$q_d = \rho_w D_w\left(\frac{\partial\alpha}{\partial y}\right)_w h_R. \quad (19)$$

Boundary conditions for (12), (17), and (15) are as follows.

At $t = 0$

$$U = V = 0. \quad (20)$$

For $s \leqq s_0$

$$\alpha = 0 \text{ for perfect catalyst,}$$
$$\alpha = \alpha_e \text{ for non-catalyst.} \quad (21)$$

For $s \geqq s_0$

$$\frac{\partial \alpha}{\partial t} = \frac{Sc}{\mu_{es} \bar{C} u_e r^{\epsilon}} (\rho k_w)\alpha. \tag{22}$$

At $t = \infty$

$$U = \frac{\alpha}{\alpha_e} = 1. \tag{23}$$

Boundary conditions (21) and (22) are derived as follows. First, for $s \leqq s_0$, $\alpha = 0$ when the surface upstream is a perfect catalyst since it is then a purely diffusion controlled reaction. Also for $s \leqq s_0$, $\alpha = \alpha_e$ when the surface upstream is non-catalytic since there is no sink for atoms. For $s \geqq s_0$, the relationship shown in (22) is derived from the fact that the diffusion rate of atoms at the wall is equal to the rate of recombination of atoms at the wall. The surface catalytic recombinations of important radicals, such as oxygen and nitrogen atoms, are known to be first order processes (see [6–11]). Thus:

$$\rho_w D_w \left(\frac{\partial \alpha}{\partial y}\right)_w = \rho_w k_w \alpha_w \tag{24}$$

where k_w is the specific reaction constant for the surface reaction and is a property of the surface material for a given gas reaction. It is directly related to the catalytic efficiency.

Finally, for $s \geqq s_0$ it should be mentioned here that the right side of the relationship in (22), strictly speaking, is not a linear function of α_w since ρ_w is also a function of α_w. In the work of [11], the equation of state of a dissociated diatomic gas was used to express ρ_w as an explicit function of α_w. The resulting non-linear boundary condition was then used for the diffusion equation, and the solutions were obtained by the use of a digital computer. In the present study, it is desired not only to obtain results of practical significance but also to have a better understanding of the governing effects of surface reaction. Attempts are therefore made to pursue the solution of the problem primarily in closed form without recourse to digital computers. For this purpose, the detailed variation of ρ_w with respect to α_w is not taken into account but, rather, ρ_w is considered a known function of pressure and surface temperature. In the light of [11], it is seen that such approximation is acceptable for practical purposes.

As it can be seen from (19) and (24), our immediate interest is to solve the diffusion equation for the surface distribution of atoms.

Two approaches to the solution of the diffusion equations is presented. Depending on the region of interest and on specific examples chosen, one of these approaches will be found to be more suitable than the other.

3. DEVELOPMENT OF A GENERALIZED VOLTERRA INTEGRAL EQUATION

One method used in the present paper to solve the diffusion equation involves a Volterra integral equation derived by combining the momentum and the diffusion equations. The development which leads to the integral equation is briefly discussed.

In [6–8], the Lighthill's heat transfer equation (reference [14]) was used to study the problem of surface reaction when k_w is invariant with respect to x. The final solution is obtained only for the flat plate. A more generalized form of the Lighthill equation was derived in [15] in connection with the boundary layer on a flat plate.

A generalized integral equation is developed here which is similar to that of [15], except that the present equation is also applicable to hypersonic blunt bodies and satisfies boundary conditions (20–23).

A comparison of the present transformed equations (12), (17), and (15), with (A15), (A16), and the homogeneous portion of (A17) of [15] shows that the present equations are mathematically identical in form to the equations of [15]. The wall boundary condition used in [15] for the energy equation was that the wall temperature is constant for $x \leqq x_0$ whereas for $x \geqq x_0$ it varies along x in a specified manner. In the present problem, for $s \leqq s_0$, α_w is constant and is equal to either zero or α_e. For $s \geqq s_0$, α_w varies along s, although it is not an *a priori* known function of s. If the relationship of (22) is left unsatisfied for the time being, it is seen from the preceding discussions that an integral equation for the surface diffusion rate of atoms can be derived in the same manner as the integral equation for heat transfer derived in [15]. Starting from (12), (17), and (15), and following the method of [15], the following generalized

integral equation is readily derived which gives the diffusion rate of atoms at the surface.

$$\left(\frac{\partial m}{\partial t}\right)_w = \gamma Sc^{1/3}\sigma(s) - \frac{Sc^{1/3}}{3^{2/3}\Gamma(4/3)\nu_{es}^{1/3}}\sqrt{[\sigma(s)]}\int_{s_0}^{s}\frac{[\mathrm{d}m_w(z)/\mathrm{d}z]\,\mathrm{d}z}{\{\int_z^s\sqrt{[\sigma(z)]}\,\mathrm{d}z\}^{1/3}} \tag{25}$$

where

$$\sigma(s) = \left(\frac{\partial U}{\partial t}\right)_w = 0{\cdot}332\,\frac{1}{\sqrt{(\nu_{es}s)}}$$

and $m \equiv \alpha/\alpha_e$.

Equation (25) combined with the boundary condition of (22) then gives, with $\xi = s/s_o$, $z = z/s_o$ and a little manipulation,

$$m_w(\xi) = A^{1/3}\Phi(\xi)\left[\gamma(0{\cdot}975)\xi^{-1/2} - \xi^{-1/4}\int_1^{\xi}\frac{[\mathrm{d}m_w(z)/\mathrm{d}z]\,\mathrm{d}z}{(\xi^{3/4} - z^{3/4})^{1/3}}\right] \tag{26}$$

where

$$A^{1/3} = \frac{(0{\cdot}332)^{1/3}}{(12)^{1/3}\Gamma(4/3)}\,Sc^{-2/3}\,C\left(\frac{u_\infty}{k_w}\right)\left(\frac{\rho_e}{\rho_w}\right)_s\left(\frac{\nu_{es}}{s_o}\right)^{1/2}L^{\epsilon},$$

$$\Phi(\xi) = \left(\frac{u_e}{u_\infty}\right)\left(\frac{r}{L}\right)^{\epsilon},$$

$$\gamma = \begin{cases}1 \text{ when } k_w \to \infty \text{ for } s \leqq s_o\\ 0 \text{ when } k_w \to 0 \text{ for } s \leqq s_o.\end{cases} \tag{27}$$

Equation (26) is a Volterra equation of the second kind. In the parameter defined in (27), k_w represents a measure of the surface reaction rate, whereas the rest of the physical quantities represent a measure of the atom diffusion rate across the boundary layer. The parameter $A^{1/3}$ is therefore essentially the ratio of a characteristic chemical reaction time to a characteristic diffusion time, and it is the reciprocal of a Damköhler number (see [9]). The function $\Phi(\xi)$ is a form factor in that it is a function only of a body shape.

The only approximation made during the entire course of deriving the Volterra integral (26) is that the velocity profile in the boundary layer was assumed to be a linear function of t (see [15]). This assumption, however, is acceptable for the analysis of a surface reaction since the atom surface distribution obtained in [6] for a uniform k_w with this assumption showed no apparent difference when compared to the atom distribution obtained by an exact numerical solution of the original differential equations.

4. METHOD OF SOLUTION OF THE VOLTERRA EQUATION

Solution of the Volterra integral equation developed in the preceding section can be obtained either by a series method or by a numerical step-by-step calculation. While the series method is more exact, its usefulness is limited. The numerical scheme used here, though involving some approximation, is general enough to adapt to all conceivable flow configurations of practical interest. Each method is outlined in the following sections.

A. *Solution by series method*

Equation (26) can be solved by a series method. Consider, first, the case of an invariant k_w all along a flat plate. For this case, $x_o = 0$, and $\gamma = 0$. If x_o is replaced by another reference length L, (26) becomes

$$m_w(\xi_1) = -A_1^{1/3}\xi_1^{-1/4}\int_0^{x/L}\frac{[\mathrm{d}m_w(z)/\mathrm{d}z]\,\mathrm{d}z}{(\xi_1^{3/4} - z^{3/4})^{1/3}} \tag{28}$$

where

$$A_1^{1/3} = \frac{(0{\cdot}332)^{1/3}Sc^{-2/3}}{(12)^{1/3}\Gamma(4/3)}\,C\left(\frac{\rho_\infty}{\rho_w}\right)\left(\frac{u_\infty}{k_w}\right)\sqrt{\left(\frac{\nu_\infty}{CLu_\infty}\right)}$$

$$\xi_1 = \frac{x}{L}.$$

Equation (28) is now essentially the same as that given in [6]. The solution of (28) was obtained in [6] by expanding m_w into a power series of $\xi_1^{1/2}$. The right side of (28) then becomes integrable and is given by a new series in powers of $\xi_1^{1/2}$ with coefficients involving Beta-functions.

Returning to the present problem, any similar attempt to integrate (26) by a straightforward expansion of $\xi^{1/2}$ fails completely, because the lower limit of the integral of (26) is not zero as was the case with (28). In order to circumvent this difficulty, a new independent variable λ is defined by

$$\lambda = \frac{4}{3}(\xi^{3/4} - 1). \tag{29}$$

The change of variable from ξ to λ transforms (26) to

$$m_w(\lambda) = A^{1/3}\Phi(\lambda)\left[\gamma(0{\cdot}975)\left(\frac{3}{4}\lambda + 1\right)^{-2/3} - \left(\frac{4}{3}\right)^{1/3}\left(\frac{3}{4}\lambda + 1\right)^{-1/3}\int_0^\lambda \frac{[\mathrm{d}m_w(z)/\mathrm{d}z]\,\mathrm{d}z}{(\lambda - z)^{1/3}}\right]. \tag{30}$$

A study of (30) shows that if m_w and Φ are expanded in the following power series,

$$m_w(\lambda) = \sum_{n=0}^{\infty} a_n \lambda^{n/3} \tag{31}$$

$$\Phi(\lambda) = \sum_{n=0}^{\infty} b_n \lambda^{n/3} \tag{32}$$

the integral appearing in (30) then becomes integrable, and the equation can be reduced to

$$\sum_{n=0}^{\infty} a_n \lambda^{n/3} = A^{1/3}\left(\sum_{n=0}^{\infty} b_n \lambda^{n/3}\right)\left\{\gamma(0{\cdot}975)\left(\tfrac{3}{4}\lambda + 1\right)^{-2/3} - \left(\tfrac{4}{3}\right)^{1/3}\left(\tfrac{3}{4}\lambda + 1\right)^{-1/3} \sum_{n=1}^{\infty} \frac{n}{3} a_n \frac{\Gamma(n/3)\,\Gamma(2/3)}{\Gamma[(n+2)/3]} \lambda^{[(n-1)/3]}\right\}. \tag{33}$$

After expanding the terms $[(3/4)\lambda + 1]^{-1/3}$ and $[(3/4)\lambda + 1]^{-2/3}$ in a power series, for $[(3/4)\lambda]^2 < 1$ the unknown constants (a_n) can be obtained from (33) by collecting the terms with like powers of λ. The resulting series (31) is then the solution of the Volterra integral equation (30) within the region of convergence of (31).

There are two limitations to the above method of solution. First, the expansions of $[(3/4)\lambda + 1]^{-1/3}$ and $[(3/4)\lambda + 1]^{-2/3}$ are valid only for $[(3/4)\lambda]^2 < 1$. Therefore, the solution of the integral equation is, at best, valid only for the region defined by $(\xi^{3/4} - 1)^2 < 1$. In addition to this limitation, the form factor expressed by (32) may cause the convergence of the series solution to be too slow for practical application of this method.

The present series method, however, gives an accurate solution of the problem within the region of convergence of the series. The results of the series method, although it may have a rather small region of convergence, can therefore be used as a check to the more approximate methods presented later in the paper. It will also be of particular interest for the case where the accurate result in a small region near $\xi = 1$ of the catalytic surface is of significance, such as a catalytic gage of small dimensions.

The series solution of the integral equation is illustrated by considering several fundamental cases. The solutions are obtained for a surface with arbitrary but constant k_w located immediately downstream of a non-catalytic leading surface ($\gamma = 0$) on a flat plate, a wedge, and a cone.

First, consider a flat plate or a wedge. The form factor Φ is unity for a flat plate and is a constant u_e/u_∞ for a supersonic wedge. Equation (33) is rewritten for a flat plate or a wedge as

$$\sum_{n=0}^{\infty} a_n \lambda^{n/3} = -\left(\tfrac{4}{3}\right)^{1/3} A^{1/3}\Phi\left(\tfrac{3}{4}\lambda + 1\right)^{-1/3} \sum_{n=1}^{\infty} \frac{n}{3} a_n \frac{\Gamma(n/3)\Gamma(2/3)}{\Gamma[(n+2)/3]} \lambda^{[(n-1)/3]}. \tag{34}$$

The solution of (34) requires an additional boundary condition with which a_o is defined. The diffusion boundary layer starts at $\lambda = 0$ and the diffusion boundary layer thickness is zero there. The only consistent m_w at such location, $\lambda = 0$, is unity (see [6] and [11]). Therefore, a_o must be unity. The other a_n's are obtained by collecting the terms with like powers of λ in (34). The determination of a_n becomes quite laborious as n increases mainly due to the term $[(3/4)\lambda + 1]^{-1/3}$. In the present study, the first twenty a_n's were obtained, of which the first nine, besides a_o, are given by

$$a_n = \frac{(-1)^n}{[\Gamma(2/3)]^n\Gamma(n/3+1)}\left(\frac{3}{4A\Phi^3}\right)^{n/3} + \frac{(-1)^{n-1}\sum_{l=3}^{n-1}(l/3)}{[\Gamma(2/3)]^{n-3}\Gamma(n/3+1)}\left(\frac{A\Phi^3}{3}\right)\left(\frac{3}{4A\Phi^3}\right)^{n/3} + \frac{(-1)^{n-1}}{[\Gamma(2/3)]^{n-6}\Gamma(n/3+1)}\left[\sum_{l=3}^{n-4}\left(\frac{l}{3}\right)\left(\frac{l+3}{3}\right) - \sum_{K=3}^{n-5}\sum_{l=K+4}^{n-1}\left(\frac{K}{3}\right)\left(\frac{l}{3}\right)\right]\left(\frac{A\Phi^3}{3}\right)^2\left(\frac{3}{4A\Phi^3}\right)^{n/3}. \quad (35)$$

The above equation is valid for $a_1 \leqq a_n \leqq a_9$ only. The remaining terms are not readily expressible in general forms and, therefore, are not given here. The surface atom distribution is then obtained by the use of (31).

Now consider the flow over an axisymmetric cone. The form factor becomes:

$$\Phi(\lambda) = \left[\left(\frac{u_e}{u_\infty}\right)\left(\frac{x_o}{L}\right)\sin\theta\right]\left(\frac{3}{4}\lambda + 1\right)^{4/9}. \quad (36)$$

In the above expression, u_e/u_∞ is constant and is a function of the free stream Mach number and the half-cone angle θ. Equation (30) becomes

$$m_w = -\left[\left(\frac{4A}{3}\right)\left(\frac{u_e}{u_\infty}\frac{x_o}{L}\sin\theta\right)^3\right]^{1/3}\left(\frac{3}{4}\lambda + 1\right)^{1/9} \int_0^\lambda \frac{(\mathrm{d}m_w/\mathrm{d}z)\,\mathrm{d}z}{(\lambda - z)^{1/3}}. \quad (37)$$

For most practical purposes $x/x_o \leqq 1{\cdot}5$ and the corresponding range of interest for λ is then about two. For such limited values of λ, the value of the term $(3/4\lambda + 1)^{1/9}$ can be considered as being practically equal to one. With this approximation, the determination of the a_n's from (37) becomes unexpectedly simple, and the surface atom distribution is obtained with the aid of (31) for all ϕ as

$$m_w = 1 + \sum_{n=1}^{\infty}\frac{(-1)^n}{[\Gamma(2/3)]^n\Gamma(n/3+1)}\phi^{n/3} \quad (38)$$

where

$$\phi = \frac{1}{[(u_e/u_\infty)(x_o/L)\sin\theta]^3}\left(\frac{3}{4A}\right)\lambda = \frac{1}{[(u_e/u_\infty)(x_o/L)\sin\theta]^3 A}(\xi^{3/4} - 1). \quad (39)$$

B. *Solution by numerical method*

It is known that a Volterra integral equation of the type given by (26) usually can be solved by a relatively simple numerical method. For instance, the availability of a numerical method of solution was suggested in [7] in connection with the Volterra equations developed for the invariant k_w cases.

A general method of solution of (26) for $\gamma = 0$ will be discussed briefly. The method will then be used to solve the problem of the reaction along a surface downstream of a non-catalytic surface for a sphere.

The Volterra integral (26) becomes, for $\gamma = 0$:

$$m_w(\xi) = -A^{1/3}\Phi(\xi)\xi^{-1/4}\int_1^\xi \frac{[\mathrm{d}m_w(z)/\mathrm{d}z]\,\mathrm{d}z}{(\xi^{3/4} - z^{3/4})^{1/3}}. \quad (40)$$

The method of solution essentially consists of subdividing the interval of interest into small sections and approximating the function $m_w(z)$ by a function such that (40) can be integrated analytically for each section. The segmentized solutions are then summed numerically, step-by-step, beginning from $\xi = 1$ so that a continuous solution of $m_w(\xi)$ can be obtained. This method of solution has the merit that it is very general in nature, and the numerical work involved is not usually excessive and can be performed by the use of a desk calculator.

The value of m_w in the nth interval is found as follows. Let the subdivision of the interval be represented by $\xi_o, \xi_1, \ldots \xi_k \ldots$ where $\xi_o = 1$ (see Fig. 2). Then, we let the solution $m_w(z)$ for the kth segment $(\xi_{k-1} \leqq z \leqq \xi_k)$ be expressed by

$$m_{w,k} = a_k - b_k z^{3/4}. \quad (41)$$

The particular exponent of z in the above equation is chosen so that (40) will be integrable

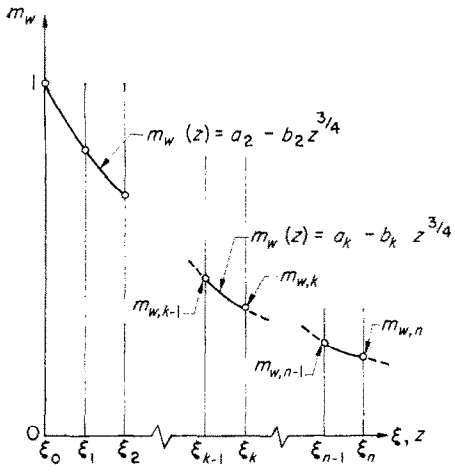

FIG. 2. The numerical method for solution of (40).

for each segment. Now for the nth segment, (40) becomes, with the aid of (41),

$$-\frac{1}{A^{1/3}}\frac{(a_n - b_n\xi_n^{3/4})\xi_n^{1/4}}{\Phi(\xi_n)} = \sum_{k=1}^{n}\left(\frac{3}{2}\right)b_k[(\xi_n^{3/4} - \xi_k^{3/4})^{2/3} - (\xi_n^{3/4} - \xi_{k-1}^{3/4})^{2/3}]. \tag{42}$$

Equation (42) has two unknowns: a_n and b_n. Another equation is obtained from the fact that m_w is continuous. For the nth segment, therefore, m_w at ξ_{n-1} must be equal to that at ξ_{n-1} obtained in the preceding segment. Therefore, we have, from (41):

$$m_{w,n-1} = a_{n-1} - b_{n-1}\xi_{n-1}^{3/4} = a_n - b_n\xi_{n-1}^{3/4}. \tag{43}$$

When a_n is eliminated from (42) and (43), there results the equation:

$$b_n = \frac{\xi_n^{1/4}m_{w,n-1} + \frac{3}{2}A^{1/3}\Phi(\xi_n)\sum_{k=1}^{n-1} b_k[(\xi_n^{3/4} - \xi_k^{3/4})^{2/3} - (\xi_n^{3/4} - \xi_{k-1}^{3/4})^{2/3}]}{\xi_n^{1/4}(\xi_n^{3/4} - \xi_{n-1}^{3/4}) + \frac{3}{2}A^{1/3}\Phi(\xi_n)(\xi_n^{3/4} - \xi_{n-1}^{3/4})^{2/3}}. \tag{44}$$

Equation (44) can be used to calculate b_n step-by-step starting from the known value of $m_{w,o} = 1$. Once b_n is obtained, a_n is calculated from (43) since $m_{w,n-1}$ is already known. $m_{w,n}$ is then obtained from (41) as

$$m_{w,n} = a_n - b_n\xi_n^{3/4}. \tag{45}$$

The method discussed above was first tested by solving the problem of surface reaction along a flat plate with an invariant k_w, the exact result of which is given in [6]. A comparison of the numerical solution with the analytical solution of [6] showed that the present numerical method gives results which are within 3 per cent of the results of [6] when $(\xi_k - \xi_{k-1}) \approx 0{\cdot}1$. Higher accuracies, when desired, may be obtained by using smaller intervals.

The numerical method has been used to solve the problem of the reaction along a surface following a non-catalytic surface on a sphere. The external hypersonic flow properties for the sphere, when taken to be the simplified ones used in [13], become

$$\left.\begin{aligned}\frac{p}{p_s} &= \cos^2\left(\frac{x}{L}\right)\\ u_e &= u_\infty\beta_s\left(\frac{x}{L}\right)\end{aligned}\right\} \text{ for } x/L \lesssim 1{\cdot}2,$$

and

$$\frac{\rho_e\mu_e}{(\rho_e\mu_e)_s} = \frac{p}{p_s}. \tag{46}$$

Results will be discussed later.

5. SOLUTION BY MODIFIED POHLHAUSEN INTEGRAL METHOD

As was seen in the preceding section, the series method, which essentially gives an exact solution, has a few fundamental limitations in its application. The numerical method, although quite flexible in its application, lacks the generality of a closed form solution. In the present section, a modified Pohlhausen integral method will be developed, which will enable us to arrive at simple, though less accurate, closed form expressions for the solutions of a flat plate and a wedge. A similar method was successfully used in [11] to solve the surface recombination problem with an invariant k_w.

The present continuity and the momentum equations, (12) and (17), and their boundary conditions in the s–t co-ordinate are mathematically identical to those for incompressible flow over a flat plate in x–y co-ordinates. The solution of the present momentum equation, therefore, can be immediately obtained from an existing solution for a flat plate with some change of variables. Using the solution given in [16], we obtain

$$\Delta = \frac{\delta}{u_\infty x_0^{\epsilon+1}} = 4{\cdot}64 \sqrt{\left(\frac{1}{Re}\frac{s_0}{u_\infty x_0^{2\epsilon+1}}\right)} \xi^{1/2} \quad (47)$$

where

$$\delta = u_e r^\epsilon \int_0^{\hat{\delta}} \frac{\rho}{\rho_{es}}\,\mathrm{d}y. \quad (48)$$

The analysis is confined to the reaction along a surface following a non-catalytic surface. The diffusion equation (15) is first integrated with respect to t, and the following integro-differential equation is derived for $\xi \geqq 1$.

$$Re\left(\frac{u_\infty x_0^{2\epsilon+1}}{s_0}\right)\frac{\mathrm{d}}{\mathrm{d}\xi}(F\Delta_m) = \frac{1}{Sc}\frac{1}{\Delta_m}\left(\frac{\partial m}{\partial \eta}\right)_w \quad (49)$$

where

$$F = \int_0^1 U(1-m)\,\mathrm{d}\eta, \quad \Delta_m = \frac{\delta_m}{u_\infty x_0^{\epsilon+1}},$$

$$\delta_m = u_e r^\epsilon \int_0^{\hat{\delta}_m} \frac{\rho}{\rho_{es}}\,\mathrm{d}y, \qquad \eta = \frac{t}{\delta_m}. \quad (50)$$

$$m = \sum_{n=0}^{5} g_n \eta^n. \quad (52)$$

The coefficients g_n are obtained by letting the profile satisfy the following boundary conditions derived from (21–23) and (15) and (7).

At $\eta = 0$

$$\frac{\partial m}{\partial \eta} = \bar{G}\Delta_m m$$

$$\frac{\partial^2 m}{\partial \eta^2} = 0. \quad (53)$$

At $\eta = 1$

$$m = 1$$

$$\frac{\partial m}{\partial \eta} = \frac{\partial^2 m}{\partial \eta^2} = 0 \quad (54)$$

where

$$\bar{G} = Sc\left(\frac{Re}{C}\right)\left(\frac{k_w}{u_\infty}\right)\left(\frac{\rho_w}{\rho_e}\right)_s\left(\frac{u_\infty}{u_e}\right)\left(\frac{x_0}{r}\right)^\epsilon. \quad (55)$$

One coefficient in (52) is left to be determined as the solution of (49); therefore, only five boundary conditions appear in (53) and (54). The concentration integral, F, given in (50) becomes

$$F = \frac{3}{14}\left(\frac{\Delta_m}{\Delta}\right)\left[1 - m_w\left(1 + \frac{4}{15}\bar{G}\Delta_m\right)\right]. \quad (56)$$

Now let us confine the remainder of the section to the analysis of flat plates and wedges. Equation (49) then becomes

$$m_w' + \frac{\frac{4}{15}\bar{G}\left(\frac{\Delta_m^2}{\Delta}\right)\Delta_m' + \left(1 + \frac{4}{15}\bar{G}\Delta_m\right)\left(\frac{\Delta_m^2}{\Delta}\right)' + \frac{14}{3}\frac{1}{Re}\frac{s_0}{u_\infty x_0 Sc}\bar{G}}{\left(\frac{\Delta_m^2}{\Delta}\right)\left(1 + \frac{4}{15}\bar{G}\Delta_m\right)} m_w = \frac{\left(\frac{\Delta_m^2}{\Delta}\right)'}{\left(\frac{\Delta_m^2}{\Delta}\right)\left(1 + \frac{4}{15}\bar{G}\Delta_m\right)}. \quad (57)$$

In order to solve (49), the U profile across the boundary layer is first approximated by a linear function

$$U = \frac{3}{2}\left(\frac{t}{\delta}\right) = \frac{3}{2}\left(\frac{\Delta_m}{\Delta}\right)\eta. \quad (51)$$

The particular coefficient 3/2 in (51) is obtained from the wall-shear calculated in [16] for a flat plate. The m-profile is approximated by the following fifth degree polynomial.

In order to solve (57) analytically, it is assumed that the thickness of the diffusion boundary layer along the present surface is the same as that along a hypothetical surface for $s \geqq s_0$ with $m_w = 0$. With this assumption Δ_m is independent of m_w, and (57) is linearized. If the boundary condition of (22) is replaced by $m_w = 0$, the present diffusion equation, (15), and its boundary condition in s–t co-ordinates becomes mathematically the same as the energy equation and

its boundary conditions analysed in [16] for a flat plate with a finite discontinuity in the surface temperature. The following equation, therefore, can be deduced from the analysis of [16];

$$\frac{\Delta_m}{\Delta} = Sc^{-1/3}(\xi^{3/4} - 1)^{1/3}\xi^{-1/4}. \tag{58}$$

Equation (57) which is now linearized by the use of (58) is solved for m_w, and the following expression is derived;

$$m_w = \frac{1}{4{\cdot}64\sqrt{\left(\frac{1}{Re}\frac{s_o}{u_\infty x_o}\right)}\,Sc^{-2/3}(\xi^{3/4}-1)^{2/3}\,[1 + G\xi^{1/4}(\xi^{3/4}-1)^{1/3}]}$$
$$\cdot \exp\left\{-\frac{14}{3(4{\cdot}64)}\bar{G}\sqrt{\left(\frac{1}{Re}\frac{s_o}{u_\infty x_o}\right)}\,Sc^{-1/3}\int\frac{d\xi}{(\xi^{3/4}-1)^{2/3}[1+G(\xi^{3/4}-1)^{1/3}\xi^{1/4}]}\right\}$$
$$\left[\frac{4{\cdot}64}{2}\sqrt{\left(\frac{1}{Re}\frac{s_o}{u_\infty x_o}\right)}\,Sc^{-2/3}\int(\xi^{3/4}-1)^{-1/3}\xi^{-1/4}\exp\left\{\frac{14\bar{G}}{3(4{\cdot}64)}Sc^{-1/3}\sqrt{\left(\frac{1}{Re}\frac{s_o}{u_\infty x_o}\right)}\right.\right.$$
$$\left.\left.\int\frac{d\xi}{(\xi^{3/4}-1)^{2/3}[1+G(\xi^{3/4}-1)^{1/3}\xi^{1/4}]}\right\}d\xi + K\right] \tag{59}$$

where K is a constant of integration, and

$$G = \frac{(4)(4{\cdot}64)}{15}Sc^{-1/3}\sqrt{\left(\frac{1}{Re}\frac{s_o}{u_\infty x_o}\right)}\bar{G}. \tag{60}$$

For a flat plate or a wedge, $s_o = Cu_e x_o$. G defined by (60) can be shown to be related to the parameter $A^{1/3}\Phi$ defined in the preceding sections by the equation

$$G = \left(\frac{4}{15}\right)(4{\cdot}64)\frac{(0{\cdot}332)^{1/3}}{(12)^{1/3}\Gamma(4/3)}\frac{1}{(A^{1/3}\Phi)}. \tag{61}$$

Equation (59) includes a single and a double integral which cannot be integrated analytically as they stand

To integrate, the integrals are divided into two parts so that each is valid in the intervals $1 \leqq \xi \leqq \xi_j$ and $\xi \geqq \xi_j$, respectively. The integrations are then performed approximately for each of the two intervals. The final solution of the problem which satisfies the boundary condition that $\lim_{\xi\to 1} m_w$ is finite is then derived from (59). The results are given as follows. For the detailed derivation of the following solution from (59) see [22].

For $1 \leqq \xi \leqq \xi_j$,

$$m_w = \frac{2(\xi^{3/4}-1)^{2/3} + 3G(\xi-1) + 4G^2I(1,\xi) + G^3[\frac{1}{5}(\xi^{3/4}-1)^{5/3} + \frac{1}{2}(\xi^{3/4}-1)^{8/3}]}{2(\xi^{3/4}-1)^{2/3}[1+G(\xi^{3/4}-1)^{1/3}\xi^{1/4}]^4}; \tag{62}$$

and for $\xi \geqq \xi_j$,

$$m_w = \frac{[(\xi^{3/4}-1)^{2/3} - (\xi_j^{3/4}-1)^{2/3} + G(\xi-\xi_j) + \frac{2}{3}G^2I(\xi_j,\xi)] + (\xi_j^{3/4}-1)^{2/3}[1+G(\xi_j^{3/4}-1)^{1/3}\xi_j^{1/4}]^3 m_{wj}}{(\xi^{3/4}-1)^{2/3}[1+G(\xi^{3/4}-1)^{1/3}\xi^{1/4}]^3} \tag{63}$$

where

$$\xi_f = 1{\cdot}333,$$

$$I(\xi_f, \xi) = \int_{(\xi_f^{3/4}-1)}^{(\xi^{3/4}-1)} z^{1/3}(1+z)^{2/3}\,dz. \quad (64)$$

Values of the integral $I(1, \xi)$ are tabulated in Table 1. It is seen that (62) and (63) are essentially closed form solutions for the flat plate and the wedge and are valid for all ξ. The accuracy of the solution is checked later by comparing it to the series solution, obtained previously, for the interval in which the series is convergent.

Table 1. Values of $I(1, \xi)$

$\xi^{3/4}-1$	$I(1, \xi) = \int_0^{\xi^{3/4}-1} z^{1/3}(1+z)^{2/3}\,dz$
0	0
0·04	0·0130
0·12	0·0461
0·24	0·1215
0·36	0·2171
0·48	0·3306
0·60	0·4609
0·72	0·6074
0·84	0·7697
0·96	0·9473
1·08	1·140
1·20	1·348
1·32	1·572
1·44	1·810
1·56	2·063
1·68	2·331

It is seen that the present solution, like the series solution, depends on the parameter G alone which is related to $A^{1/3}\Phi$ by (61).

6. HEAT TRANSFER

Total heat transfer to a surface upon which the atoms are recombining is given by (18).

$$q_T = q_c + q_d. \quad (18)$$

In the above equation, q_c is the heat transfer due to the convection of frozen thermal and kinetic energy, and q_d is that due to the diffusion of atoms and their recombination at the surface. Solution of the energy equation (14) and thus q_c was obtained in [13] as

$$q_c = 0{\cdot}47Pr^{-2/3}\sqrt{[(\rho_e\mu_e)_s C]}\sqrt{(u_\infty)}(h_e - h_w)\Omega(x) \quad (65)$$

where

$$\Omega(x) = \frac{\dfrac{1}{\sqrt{(2)}}\dfrac{\rho_e\mu_e}{(\rho_e\mu_e)_s}\dfrac{u_e}{u_\infty}r^\epsilon}{\left[\displaystyle\int_0^x \frac{\rho_e\mu_e}{(\rho_e\mu_e)_s}\left(\frac{u_e}{u_\infty}\right)r^{2\epsilon}\,dx\right]^{1/2}}. \quad (66)$$

The quantity q_d can be obtained from (19) and (24), and the values of $m_w(x)$ can be obtained from the solutions of the diffusion equations described in the preceding sections. In particular,

$$q_d = \rho_w k_w a_e m_w h_R, \quad (67)$$

for $x \geqq x_o$.

For the specific problems solved in the present analysis, q_d is zero for $x \leqq x_o$ because $\gamma = 0$.

7. RESULTS AND DISCUSSION

The results of the analysis will be discussed first. Some of the implications of the results to two specific applications mentioned in the introduction of the paper will then be studied.

A. *General results of analysis*

Results have been obtained for configurations wherein the surface of finite catalytic efficiency is displaced downstream from the leading edge or the stagnation point. The surface in the front portion is assumed to be non-catalytic. The effects of this displacement are studied by comparing the present solutions with the existing solutions for the same body geometry but with uniform surface catalytic efficiency. For simplicity, we shall denote the two configurations as the displaced catalytic surface and uniform catalytic surface cases, respectively. Surface distribution of atoms on the displaced catalytic surface for a flat plate or a wedge is shown on Fig. 3. The solid lines show the values calculated by the use of (62) and (63). The points are the values calculated from the series solution of (31) and (35). The limited comparison given in the figure between the solid lines and the points shows that the results of the integral method are quite acceptable for practical purposes.

The broken lines in Fig. 3 are for the corresponding uniform catalytic surface cases obtained from [6]. It is seen that the present m_w decreases rather rapidly up to ξ of about 1·1; however, it levels off quite sharply and then

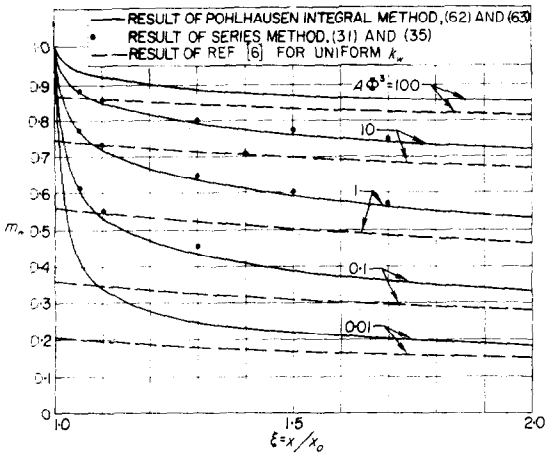

FIG. 3. Surface distribution of atoms over flat plate and supersonic wedge.

approaches the broken line asymptotically. Thus, the atom concentrations along the displaced catalytic surface stay substantially above the values for the uniform catalytic case for a considerable length of the surface. This means, as seen from (19) and (24), that the effect of having a non-catalytic surface upstream is to increase q_d along the downstream surfaces with a finite catalytic efficiency.

Fig. 4 shows the surface distributions of atoms around a spherical nose computed numerically by the use of (40–46). The solid lines show the variation of m_w along a displaced catalytic surface starting from $x/L = 0{\cdot}6$. The broken lines, on the other hand, show the values of m_w for the uniform catalytic surface obtained from the analysis of [11]. The general relative behavior of the two cases are seen to be similar to that for the flat plate or the wedge. The abscissa of Fig. 4 is x/L rather than ξ as used in Fig. 3. This is because the problem for the sphere had to be solved separately for each x_0.

The effect of a non-catalytic upstream surface on the chemical reaction along a catalytic surface is seen from Figs. 5 and 6 for the flat plate or wedge and the sphere, respectively. The figures show the parameter $m_w/(m_w)_{un}$. The rate at which the chemical reaction is taking place at a surface is directly proportional to m_w as is seen in (19) and (24). The quantity $m_w/(m_w)_{un}$, therefore, represents the ratio of the chemical reaction rate along the present surface to that

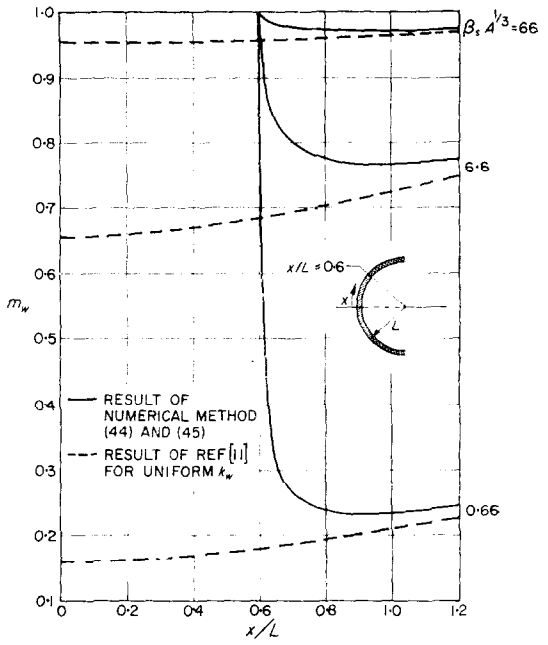

FIG. 4. Surface distribution of atoms around spherical nose.

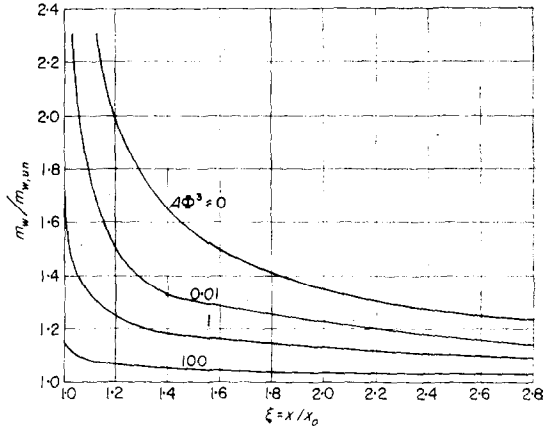

FIG. 5. Decay of upstream surface effect over flat plate and wedge.

of the uniform catalytic surface. When the boundary layer and the surface reaction forget completely the existence of the non-catalytic upstream surface, the ratio $m_w/(m_w)_{un}$ is expected to eventually become unity.

Fig. 5 shows that for a flat plate or a wedge m_w approaches $(m_w)_{un}$ faster as the parameter

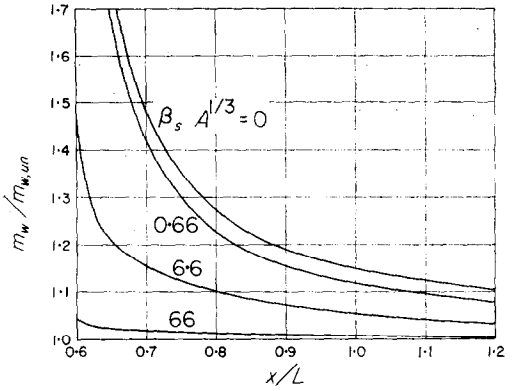

FIG. 6. Decay of upstream surface effect around spherical nose.

$A\Phi^3$ is increased. In the limit, as $A\Phi^3 \to \infty$, $m_w/(m_w)_{un} = 1$ for all $x \geqq x_o$. Since $A \sim 1/k_w$, $A\Phi^3 \to \infty$ implies that the surface for $x \geqq x_o$, like the upstream surface, is non-catalytic and, therefore, there is no discontinuity at $x = x_o$, consequently, there are no adjustments to be made by the boundary layer or the surface reaction. The longest time for m_w to reach $(m_w)_{un}$ is required when $A\Phi^3 = 0$, which is the case when the surface at $x = x_o$ varies from a non-catalyst to a perfect catalyst. It is also seen in the figure that for most of the finite k_w considered, m_w reaches a value within 20 per cent of $(m_w)_{un}$ in the length of about one x_o. A qualitatively similar trend is apparent for the sphere in Fig. 6. The m_w for $x \geqq x_o$, however, approaches $(m_w)_{un}$ much faster as a whole than it did along a flat plate or a wedge. This is to be expected, since both the favorable pressure gradient and the three dimensionality associated with the sphere would tend to keep the boundary layer thinner. The behavior of the boundary layer for $x \geqq x_o$, therefore, recovers much faster to that over a uniform catalytic surface.

The solution for the cone, (38), is plotted in Fig. 7. It is seen that the entire solution for the cone depends on one variable, ϕ. Since the general behavior of the chemical reaction rate and the boundary layer for $x \geqq x_o$ is essentially similar to that for the wedges and spheres, no particular discussion of this configuration is necessary.

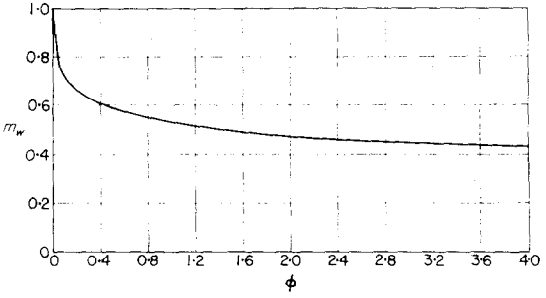

FIG. 7. Surface distribution of atoms over supersonic cone.

B. *Local reduction of heat transfer by the use of a non-catalyst*

As shown in Figs. 3–6, atom concentrations along the displaced catalytic surface stay above the values for the uniform catalytic surface for a considerable length of the surface. Since q_d is directly proportional to m_w, the effect of having a non-catalytic surface upstream is to increase q_d along the downstream catalytic surfaces.

Let us suppose that we wish to reduce the local heat transfer at a location, where the heat transfer is normally high, by making the surface locally non-catalytic. Then the present analysis indicates that we would be reducing the local heat transfer at the expense of increasing the heat transfer along the catalytic surfaces immediately downstream.

This phenomenon is seen more clearly in Fig. 8. In the upper portion of the figure, the broken line shows the total heat transfer along the uniform catalytic surface for a flat plate or a wedge. The solid line shows the total heat transfer along the displaced catalytic surface located downstream of $\xi = 1$. A comparison of the two lines shows that the heat transfer is decreased along the upstream surface, but at the same time, it is increased along the downstream surface. The physical reasoning is given as follows: as the upstream surface is made non-catalytic, the reactant accumulates excessively along the surface. As soon as the catalytic surface is reached at $\xi = 1$, the surface reaction is suddenly permitted, and it proceeds at a much greater rate than that for the uniform catalytic surface, since no excess accumulation of the

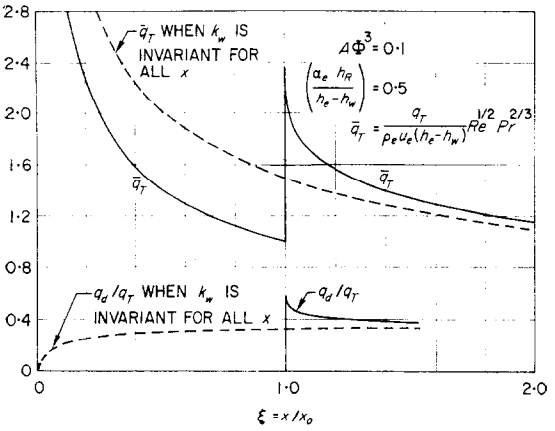

FIG. 8. Effect of non-catalytic upstream surface on heat transfer to downstream for $Pr/Sc = 1{\cdot}4$.

reactant is present in the latter case. In contrast to other means of reduction of local heat transfer, such as the scheme of localized mass transfer, the reduction of heat transfer by making the surface non-catalytic, therefore, has an adverse effect on heat transfer over the downstream surfaces of finite catalycity. In the case of a localized mass transfer, it is known that an appreciable reduction of heat transfer can be obtained for the downstream surfaces as well (see [15]). However, because of the severe limitation normally imposed upon the level of heat transfer near the stagnation point, mainly from material consideration, an alleviation of heat transfer at this point, even at the expense of creating regions of high heat flux downstream, may still prove advantageous in many practical applications.

The differences of heat transfers shown by the solid and the broken lines for $\xi \geqq 1$ vary directly with $\alpha_e h_R/(h_e - h_w)$. It also increases as the parameter $A\Phi^3$ is decreased.

C. *Application to the differential gage for high temperature facility diagnostics*

Several forms of the differential gage have been proposed and used to measure the stream concentration of dissociated atoms in high temperature test facilities (see [17] and [18]). The basic principle of operation of the gage consists of locating a pair of non-catalytic and highly catalytic surfaces in such a way that the flow configurations over the surfaces are identical. The measured heat transfer to the non-catalytic surface gives q_c, whereas the measured heat transfer to the catalytic surfaces give $q_T = q_c + q_d$. The difference of the two would give q_d from which α_w may be obtained from (19) and (24). The solutions of the diffusion equation for the surface reactions such as those given in the present paper give α_w as a function of α_e when the gas phase reaction is frozen. With known α_w, α_e may be obtained from these solutions, and α_e is the same as α_∞.

It is seen from the brief discussion given above that there are two basic conditions which must be satisfied for a successful operation of the gage. First, the gas-phase chemical reaction should be completely frozen. The stagnation region of a blunt body may be an ideal location for the gage surfaces from the viewpoint of actual construction and also from the fact that the theory of the stagnation point boundary layer with the catalytic surface reaction is much better established than that for other flow configurations [19]. One can see, however, from the analyses of gas-phase chemical reaction near the stagnation region given in references [2]–[4], [20], and [21] that one may have to reduce the nose radius to a much smaller size than would be feasible for a particular application in order to freeze the gas-phase reaction. Also, in many cases when the free stream Mach number is high, the reduction of the nose size may take the flow out of the boundary layer regime so that the validity of analysis based on the boundary layer theory may become questionable.

Such difficulties may be circumvented either by locating the gage surfaces sufficiently away from the stagnation point on a blunt body or by using a wedge or a flat plate instead. As can be seen from the non-equilibrium boundary layer analysis of [3], the boundary layer reaction freezes rapidly as the gas flows around a blunt body. The reaction in the gas outside the blunt body boundary layer probably would freeze even faster since the velocity and the temperature are higher there than in the boundary layer. Also, the gas-phase chemical reaction usually freezes much more readily on a wedge or a flat plate than near the stagnation region of a blunt body. This follows because the pressure is much

lower and the flow velocities are much higher along the surface of a wedge, for instance, than at the stagnation region. Furthermore, it may be advantageous from the engineering standpoint to install the gage surfaces away from the leading edge of a flat plate or a wedge. It is then seen that the present analysis can be used to deduce α_e when the gage surfaces are not located at stagnation points or at leading edges.

The next condition which is required in order to operate the gages satisfactorily is that one of the gage surfaces be non-catalytic whereas the other highly catalytic. In order to deduce an accurate value of α_e from the heat transfer measurements, the ratio, q_d/q_T obtained must be as large as possible. The ratio, q_d/q_T is plotted at the lower portion of Fig. 8 for the flat plate and the wedge. The plot is for $\alpha_e h_R/(h_e - h_w)$ of 0·5 and $A\Phi^3 = 0{\cdot}1$. The solid line is for the surface of $x \geqq x_o$ which is preceded by a non-catalytic surface. The broken line is for the uniform catalytic surface which has the same finite k_w from the leading edge. The results show that the ratio q_d/q_T, which is a measure of the sensitivity of the gages, is increased as the gage surfaces are preceded by a non-catalytic surface.

A comparison is made of the ratio q_d/q_T between the gage surfaces located flush with the leading edge and those located away from the edge. For the flow conditions corresponding to the results of Fig. 8, let us assume that the latter gages are located 3 in away from the leading edge ($x_o = 3$ in), and both gages are 0·9 inches in streamwise length. Then the integration under the appropriate q_d/q_T curves shows that the over-all ratio of q_d and q_T is increased by about 100 per cent as the gages are simply moved downstream 3 in. It is seen, therefore, that the sensitivity of a given gage could be increased by making the surface preceding the gage non-catalytic. For gages of smaller length, the increase in the over-all ratio of q_d and q_T is even more pronounced. Similar arguments apply to other body shapes such as the cone and the sphere.

8. CONCLUDING REMARKS

The catalytic recombination of atoms along a surface with a discontinuous variation of the surface catalycity is studied. The catalycity is considered to have a discrete jump from either zero or infinity to an arbitrarily constant value at a given location. Highly-cooled hypersonic boundary layers are considered for general two-dimensional and axisymmetric bodies. Two approaches are used in the study. One involves a Volterra integral equation which is solved by both a series method and a numerical method. The other uses a modified Pohlhausen integral method.

Since the Volterra equation is derived with the only assumption of a linear velocity profile it is expected to be more accurate than the Pohlhausen method where additional assumption is made on the concentration profile. When accurate local value of m_w is desired, such as in the application of flow diagnostics, the Volterra method is to be preferred. In the study of over-all heat transfer in terms of governing parameters, however, the closed form solution given by the Pohlhausen method is more useful.

Specific solutions are obtained for the case of k_w varying from zero to an arbitrarily constant value on the surface of flat plates, wedges cones, and spherical noses. Analytical solutions of the diffusion equation are obtained for the flat plate, wedges, and the cones. The numerical method, on the other hand, is used to obtain a solution around the spherical nose.

The results show that having a non-catalytic upstream surface increases the heat transfer along a downstream surface with a given finite k_w. This increase could be considerable depending on the Damköhler number. Therefore, when a non-catalytic surface is used to reduce a local heat transfer, it is done at the expense of increasing the heat transfer to the catalytic surfaces following the non-catalytic surface.

It was shown, through the analysis, that the sensitivity of a double-surface gage could be increased considerably by preceding the catalytic gage surface by a non-catalytic surface.

The present analysis was based on a boundary layer theory. It, therefore, does not strictly apply near $x = x_o$ where the discontinuity in k_w occurs. The nature of the atom diffusion at $x = x_o$ is similar to that of the heat convection at a point where a sudden variation in wall temperature occurs, but it is not as drastic since here m_w does not have a discontinuity at $x = x_o$. The inadequacy of the boundary layer theory

at $x = x_0$, however, should not have any appreciable effect for $x > x_0$.

In closing, it might be mentioned that, though only the discontinuous variations of k_w have been considered in the present analysis, the present methods can also be used to solve the case of continuous variation in k_w. As a matter of fact, the solutions for the continuously varying k_w can be obtained in a simpler manner. This case and other related cases will be presented in a future paper.

REFERENCES

1. D. E. ROSNER, Aeronautical Research Laboratory, Wright–Patterson Air Force Base, Dayton, Ohio, Part 1, 99 (1961).
2. J. A. FAY and F. R. RIDDELL, *J. Aero. Sci.* **25**, 73, 121 (1958).
3. P. M. CHUNG and A. D. ANDERSON, Proc. Heat Transfer and Fluid Mech. Inst. 150 (1960).
4. G. GOODWIN and P. M. CHUNG, *Advanc. Aero. Sci.* **4**, 997 (1961).
5. S. M. SCALA, Proc. U.S. *Nat. Congr. Appl. Mech.* 799 (1958).
6. P. L. CHAMBRÉ and A. ACRINOS, *J. Appl. Phys.* **27**, 1322 (1956).
7. P. L. CHAMBRÉ, *Appl. Sci. Res.* **A6**, 97 (1956).
8. A. ACRINOS and P. L. CHAMBRÉ, *Industr. Engng. Chem.* **49**, 1025 (1957).
9. D. E. ROSNER, *J. Aero/Space Sci.* **26**, 281 (1959).
10. D. E. ROSNER, Tech. Pub. No. 14, Aero. Chem. Res. Labs., Inc., Princeton, N.J. (1959). Also *A.I.Ch.E.* Preprint No. 135 (1961).
11. P. M. CHUNG and A. D. ANDERSON, *N.A.S.A.* TN D-350 (1961).
12. L. LEES, *Third AGARD Combustion and Propulsion Panel Coloquium*, p. 451. Pergamon Press, New York (1959).
13. L. LEES, *Jet Propulsion*, **26**, 259 (1956).
14. M. J. LIGHTHILL, *Proc. Roy. Soc.* A, **202**, 359 (1950).
15. M. W. RUBESIN and M. INOUYE, *N.A.C.A.* TN 3969 (1957).
16. E. R. G. ECKERT, *Introduction to the Transfer of Heat and Mass*. McGraw-Hill, New York (1950).
17. D. E. ROSNER, *J. Amer. Rocket Soc.* **32**, 1065 (1962).
18. E. L. WINKLER and R. N. GRIFFIN, *N.A.S.A.* TN D-1146 (1961).
19. R. J. GOULARD, *Jet Propulsion*, **28**, 737 (1958).
20. P. M. CHUNG, *N.A.S.A.* TR 109 (1961).
21. R. A. HARTUNIAN and P. V. MARRONE, Cornell Aero Labs., Report No. AD-1118-A-7 (1959).
22. P. M. CHUNG, S. W. LIU and H. MIRELS, Aerospace Corp. Report No. TDR-69 (2240–20) TN-1 (1962).

Résumé—On étudie la recombinaison catalytique des atomes le long d'une paroi dont le pouvoir catalytique est discontinu. On considère la cas où ce pouvoir catalytique fait, en un point donné, un léger saut, à partir de zéro ou de l'infini, jusqu'à une valeur quelconque mais constante. On étudie les couches limites hypersoniques très refroidies sur des corps à deux dimensions ou des corps de révolution. Deux méthodes sont envisagées pour cette étude, l'une utilise l'équation intégrale de Volterra, résolue à la fois par mise en série et par une méthode numérique, l'autre utilise l'équation de Pohlhausen modifiée.

On étudie l'effet, d'une surface amont non catalytique, sur la transmission de chaleur vers les surfaces aval dont le pouvoir catalytique est défini. On propose également une méthode pour accroître la sensibilité d'une jauge catalytique différentielle utilisée pour déterminer les concentrations locales en atomes dans les dispositifs expérimentaux à haute température.

Zusammenfassung—Die katalytische Rekombination von Atomen entlang einer Oberfläche mit diskontinuierlicher Veränderung der katalytischen Oberflächenaktivität wird untersucht. Man nimmt an, dass die katalytische Wirkung einen Sprung von Null oder Unendlich auf beliebige aber konstante Werte an einer bestimmten Stelle aufweist. Stark gekühlte hypersonische Laminargrenzschichten werden für allgemeine zwei-dimensionale achssymmetrische Körper untersucht. Die Untersuchung stützt sich auf zwei Näherungsmöglichkeiten: einer Volterra-Integralgleichung, die sowohl nach einer Reihenmethode, als auch nach einer numerischen Methode gelöst wurde und einer modifizierten Pohlhausen Integralmethode.

Der Einfluss einer nicht katalytisch wirkenden Anlaufstrecke auf den Wärmeübergang an eine stromabwärts gelegene Fläche von endlicher katalytischer Wirkung wird diskutiert. Auch liess sich eine Methode vervollkommnen, um die Empfindlichkeit von differentialkatalytischen Messvorrichtungen zu erhöhen, die zur Bestimmung von örtlichen Atomkonzentrationen in Hochtemperaturversuchseinrichtungen dienen.

Аннотация—Исследуется каталитическая рекомбинация атомов вдоль поверхности при нарушении непрерывности каталитической активности последней. Считается, что каталитическая активность имеет дискретный скачок от нуля или бесконечности до произвольной, но постоянной величины в заданном положении. Рассматриваются сильно охлажденные сверхзвуковые ламинарные пограничные слои у обычных двумерных и

o

осесимметричных тел. При исследовании использовались два подхода: интегральное уравнение Вольтерра, решаемое как методом разложения в ряд, так и численным методом, и модифицированный интегральный метод Польхаузена.

Рассматривается влияние некаталитической поверхности вверх по течению на перенос тепла к поверхностям вниз по течению с конечной каталитической активностью. Предложен способ усиления чувствительности дифференциального каталитического измерительного прибора, используемого для определения локальной атомной концентрации в высокотемпературных экспериментальных установках.